

Sirt3 Mediates Reduction of Oxidative Damage and Prevention of Age-Related Hearing Loss under Caloric Restriction

Shinichi Someya,^{1,3,5} Wei Yu,^{2,5} William C. Hallows,² Jinze Xu,⁴ James M. Vann,¹ Christiaan Leeuwenburgh,⁴ Masaru Tanokura,³ John M. Denu,^{2,*} and Tomas A. Prolla^{1,*}

¹Departments of Genetics and Medical Genetics

²Department of Biomolecular Chemistry

University of Wisconsin, Madison, WI 53706, USA

³Department of Applied Biological Chemistry, University of Tokyo, Yayoi, Tokyo 113-8657, Japan

⁴Department of Aging and Geriatrics and The Institute on Aging, University of Florida, Gainesville, FL 32611, USA

⁵These authors contributed equally to this work

*Correspondence: jmdenu@wisc.edu (J.M.D.), taprolla@wisc.edu (T.A.P.)

DOI 10.1016/j.cell.2010.10.002

SUMMARY

Caloric restriction (CR) extends the life span and health span of a variety of species and slows the progression of age-related hearing loss (AHL), a common age-related disorder associated with oxidative stress. Here, we report that CR reduces oxidative DNA damage in multiple tissues and prevents AHL in wild-type mice but fails to modify these phenotypes in mice lacking the mitochondrial deacetylase Sirt3, a member of the sirtuin family. In response to CR, Sirt3 directly deacetylates and activates mitochondrial isocitrate dehydrogenase 2 (Idh2), leading to increased NADPH levels and an increased ratio of reduced-to-oxidized glutathione in mitochondria. In cultured cells, overexpression of Sirt3 and/or Idh2 increases NADPH levels and protects from oxidative stress-induced cell death. Therefore, our findings identify Sirt3 as an essential player in enhancing the mitochondrial glutathione antioxidant defense system during CR and suggest that Sirt3-dependent mitochondrial adaptations may be a central mechanism of aging retardation in mammals.

INTRODUCTION

It is well established that reducing food consumption by 25%–60% without malnutrition consistently extends both the mean and maximum life span of rodents (Weindruch and Walford, 1988; Koubova and Guarente, 2003). Caloric restriction (CR) is also known to extend life span in yeast, worms, fruit flies, spiders, birds, and monkeys and delays the progression of a variety of age-associated diseases such as cancer, diabetes, cataract, and age-related hearing loss (AHL) in mammals (Wein-

druch and Walford, 1988; Sohal and Weindruch, 1996; Someya et al., 2007; Colman et al., 2009). Furthermore, CR reduces neurodegeneration in animal models of Parkinson's disease (Mattson, 2000) as well as Alzheimer's disease (Zhu et al., 1999). The mitochondrial free radical theory of aging postulates that aging results from accumulated oxidative damage caused by reactive oxygen species (ROS), originating from the mitochondrial respiratory chain (Balaban et al., 2005). Consistent with this hypothesis, mitochondria are a major source of ROS and of ROS-induced oxidative damage, and mitochondrial function declines during aging (Wallace, 2005). A large body of evidence suggests that CR reduces the age-associated accumulation of oxidatively damaged proteins, lipids, and DNA through reduction of oxidative damage to these macromolecules and/or enhanced antioxidant defenses to oxidative stress (Weindruch and Walford, 1988; Sohal and Weindruch, 1996; Masoro, 2000). Yet, whether the anti-aging action of CR in mammals is a regulated process and requires specific regulatory proteins such as sirtuins still remains unclear.

Sirtuins are NAD⁺-dependent protein deacetylases that regulate life span in lower organisms and have emerged as broad regulators of cellular fate and mammalian physiology (Donmez and Guarente, 2010; Finkel et al., 2009). A previous report has shown that life span extension by CR in yeast requires Sir2, a member of the sirtuin family (Lin et al., 2000), linking sirtuins and CR-mediated retardation of aging. In mammals, there are seven sirtuins that display diverse cellular localization (Donmez and Guarente, 2010; Finkel et al., 2009). Previous studies have focused on the role of Sirt1 as the major sirtuin mediating the metabolic effects of CR in mammals (Chen et al., 2005; Bordonie et al., 2007; Chen et al., 2008). However, recent studies indicate that upregulation of Sirt1 in response to CR is not observed in all tissues examined (Cohen et al., 2004; Barger et al., 2008), and currently, no study has provided conclusive evidence that sirtuins play an essential role in CR-mediated aging retardation in mammals. Sirt3 is a member of the mammalian sirtuin family that is localized to mitochondria and

regulates levels of ATP and the activity of complex I of the electron transport chain (Ahn et al., 2008) and, as such, may play a role in the metabolic reprogramming mediated by CR. A recent study has shown that CR increases Sirt3 levels in liver mitochondria (Schwer et al., 2009). Fasting also increases Sirt3 protein expression in liver mitochondria, and mice lacking Sirt3 display the hallmarks of fatty acid oxidation disorders, indicating that Sirt3 modulates mitochondrial fatty acid oxidation in mammals (Hirschey et al., 2010). Furthermore, CR increases expression of Sirt3 in primary mouse cardiomyocytes, whereas overexpression of *Sirt3* protects these cells from oxidative stress-induced cell death (Sundaresan et al., 2008), suggesting a potential role of Sirt3 in the aging retardation associated with CR in mammals.

AHL is a universal feature of mammalian aging and is the most common sensory disorder in the elderly (Someya and Prolla, 2010; Liu and Yan, 2007). AHL is characterized by an age-associated decline of hearing function associated with loss of spiral ganglion neurons and sensory hair cells in the cochlea of the inner ear (Someya and Prolla, 2010; Liu and Yan, 2007). The progressive loss of neurons and hair cells in the inner ear leads to the onset of AHL because these postmitotic cells do not regenerate in mammals. The onset of AHL begins in the high-frequency region and spreads toward the low-frequency region during aging (Keithley et al., 2004; Hunter and Willott, 1987). This is accompanied by the loss of neurons and hair cells beginning in the basal region and spreading toward the apex of the cochlea of the inner ear with age. A previous study has shown that CR slows the progression of AHL in CBA/J mice (Sweet et al., 1988), whereas we have shown previously that CR prevents AHL in C57BL/6J mice, reduces cochlear degeneration, and induces *Sirt3* in the cochlea (Someya et al., 2007). Both strains of mice have been extensively used as a model of AHL, although the age of onset of AHL varies from 12–15 months of age in C57BL/6J mice to 18–22 months of age in CBA/J mice (Zheng et al., 1999). Experimental evidence suggests that oxidative stress plays a major role in AHL (Jiang et al., 2007; Someya et al., 2009) and that CR protects cochlear cells through reduction of oxidative damage and/or by enhancing cellular antioxidant defenses to oxidative stress (Someya et al., 2007). Yet, the molecular mechanisms by which CR reduces oxidative cochlear cell damage remain unknown.

In this report, we show that the mitochondrial deacetylase Sirt3 is required for the CR-mediated prevention of AHL in mice. We also show that Sirt3 is required for the reduction of oxidative damage in multiple tissues under CR conditions, as evidenced by DNA damage levels. At the mechanistic level, Sirt3 directly deacetylates isocitrate dehydrogenase 2 (Idh2), an enzyme that converts NADP⁺ to NADPH in mitochondria. In response to CR, Sirt3 stimulates Idh2 activity in mitochondria, leading to increased levels of NADPH and an increased ratio of reduced glutathione/oxidized glutathione, the major redox couple in the cell. In cultured cells, overexpression of Sirt3 and/or Idh2 increases NADPH levels and protects these cells from oxidative stress. The data presented here provide the first conclusive evidence that CR-mediated reduction of oxidative damage and prevention of a common age-related

phenotype (AHL) require a member of the sirtuin family in mammals.

RESULTS

Sirt3 Is Required for the CR-Mediated Prevention of Age-Related Cochlear Cell Death and Hearing Loss

First, to investigate whether Sirt3 plays a role in the CR prevention of AHL, we conducted a 10 month CR dietary study using WT and *Sirt3*^{-/-} mice that have been backcrossed onto the C57BL/6J background. The C57BL/6J strain is considered an excellent model to study the anti-aging action of CR because this mouse strain is the most widely used mouse model for the study of aging and responds to CR with a robust extension of life span (Weindruch and Walford, 1988) and prevention of AHL (Someya et al., 2007). We reduced the calorie intake of WT and *Sirt3*^{-/-} mice to 75% (a 25% CR) of that fed to control diet (CD) mice in early adulthood (2 months of age), and this dietary regimen was maintained until 12 months of age. The auditory brainstem response (ABR), a common electrophysiological test of hearing function, was used to monitor the progression of AHL in these mice (Someya et al., 2009). We first confirmed that aging resulted in increased ABR hearing thresholds at the high (32 kHz), middle (16 kHz), and low (8 kHz) frequencies in 12-month-old WT mice (Figure 1A), indicating that these mice displayed hearing loss. As predicted, CR delayed the progression of AHL at all tested frequencies in WT mice (Figure 1A). Strikingly, CR did not delay the progression of AHL in *Sirt3*^{-/-} mice (Figure 1A), although CR had the same effect on body weight reduction in both WT and *Sirt3*^{-/-} mice (Figures S2A and S2B available online). Neural and hair cell degeneration are hallmarks of AHL (Keithley et al., 2004). In agreement with the hearing test results, basal regions of the cochleae from calorie-restricted WT mice displayed only minor loss of spiral ganglion neurons (Figures 1J and 1K; see also Figures 1B, 1C, 1F and 1G) and hair cells (Figure S1E; see also Figures S1A and S1C), whereas CR failed to protect these cells in *Sirt3*^{-/-} mice (Figures 1L and 1M; see also Figures 1D, 1E, 1H, and 1I; Figure S1F; see also Figures S1B and S1D). Collectively, these results demonstrate that Sirt3 plays an essential role in the CR-mediated prevention of age-related cochlear cell death and hearing loss in mice.

Next, to investigate whether Sirt3 plays a role in the metabolic effects induced by CR, we conducted a 3 month CR dietary study using WT and *Sirt3*^{-/-} mice starting at 2 months of age. Mice lacking the *Sirt3* gene appeared phenotypically normal under basal and CR conditions: *Sirt3*^{-/-} mice were viable and fertile, and no significant changes were observed in body weight (Figures S2A and S2B), bone mineral density (Figure S2C), body fat (Figure S2D), tissue weight (Figure S2E), serum glucose levels (Figure S3A), glucose tolerance (Figure S3B), serum Igf-1 (Figure S3C), and cholesterol (Figure S3D) levels between control diet WT and *Sirt3*^{-/-} mice or calorie-restricted WT and *Sirt3*^{-/-} mice at 5 months of age. However, though we found that WT mice displayed lower levels of serum insulin (Figure S3E) and triglycerides (Figure S3F) in response to CR, no significant changes were observed in these serum markers between control diet-fed and calorie-restricted *Sirt3*^{-/-}

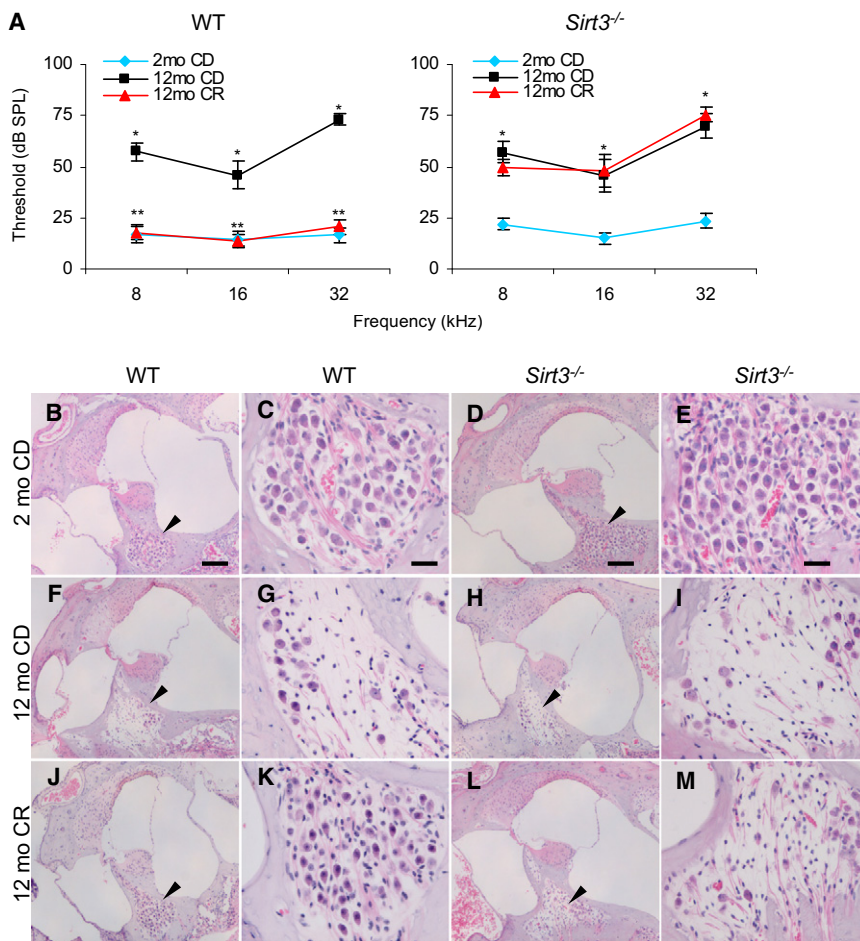


Figure 1. CR Prevents AHL and Protects Cochlear Neurons in WT Mice, but Not in *Sirt3*^{-/-} Mice

(A) ABR hearing thresholds were measured at 32, 16, and 8 kHz from control diet and/or calorie-restricted WT (left) and *Sirt3*^{-/-} (right) mice at 2 and 12 months of age (n = 9–12). *Significantly different from 2-month-old WT or *Sirt3*^{-/-} mice (p < 0.05), **significantly different from 12-month-old WT mice (p < 0.05). CD, control diet; CR, calorie restricted diet.

(B–M) Neurons in the basal cochlear regions from WT mice in control diet at 2 (B and C) and 12 (F and G) months of age and calorie-restricted diet at 12 months of age (J and K). Neurons from control diet *Sirt3*^{-/-} mice at 2 (D and E) and 12 (H and I) months of age and calorie-restricted *Sirt3*^{-/-} mice at 12 months of age (L and M) (n = 5). Arrows in the lower-magnification photos indicate neuron regions. Scale bars, 100 μ m (B, F, J, D, H, and L) and 20 μ m (C, G, I, E, I, and M). Data are means \pm SEM. See also Figure S1, Figure S2, and Figure S3.

mice (Figures 2C–2E). Together, these results provide evidence that Sirt3 plays an essential role in the CR-mediated reduction of oxidative DNA damage in multiple tissues.

Sirt3 Enhances the Mitochondrial Glutathione Antioxidant Defense System in Response to CR

A previous study has shown that overexpression of *Sirt3* increased mRNA expression of the antioxidant genes

mice, suggesting a possible role of Sirt3 in metabolic adaptations to CR.

Sirt3 Is Required for the CR-Mediated Reduction of Oxidative Damage in Multiple Tissues

How does Sirt3 reduce cochlear cell degeneration and slow the progression of AHL in response to CR? It is well established that CR reduces oxidative damage to DNA, proteins, and lipids in multiple tissues in mammals (Sohal and Weindruch, 1996; Masoro, 2000; Hamilton et al., 2001). Hence, we hypothesized that Sirt3 may play a role in the CR-mediated reduction of oxidative damage in the cochlea and other tissues. To test this hypothesis, we measured oxidative damage to DNA in the cochleae, brain (neocortex), and liver of control diet and calorie-restricted WT and *Sirt3*^{-/-} mice at 12 months of age. We found that CR reduced oxidative DNA damage in WT mice, as determined by measurements of 8-hydroxyguanosine and apurinic/aprimidinic (AP) sites, but failed to reduce oxidative DNA damage in tissues from *Sirt3*^{-/-} mice (Figures 2A and 2B). In agreement with the oxidative damage results, CR increased spiral ganglion neuron survival (Figure 2C), outer hair cell survival (Figure 2D), and inner hair cell survival (Figure 2E) in the basal regions of the cochleae of WT mice, whereas CR failed to protect these cells in *Sirt3*^{-/-}

manganese superoxide dismutase (*MnSOD*) and catalase (*Cat*) in primary cardiomyocytes and that *Sirt3*^{-/-} primary cardiomyocytes displayed higher levels of ROS compared to those of WT cells (Sundaresan et al., 2009), suggesting that Sirt3 may regulate the antioxidant systems. Glutathione acts as the major small molecule antioxidant in cells (Anderson, 1998; Halliwell and Gutteridge, 2007; Marí et al., 2009; Rebrin et al., 2003), and NADPH-dependent glutathione reductase regenerates reduced glutathione (GSH) from oxidized glutathione (GSSG) (Anderson, 1998; Marí et al., 2009). In healthy mitochondria from young mice, glutathione is found mostly in the reduced form, GSH (Marí et al., 2009). During aging, oxidized glutathione accumulates, and hence an altered ratio of mitochondrial GSH to GSSG is thought to be a marker of both oxidative stress and aging (Rebrin et al., 2003; Schafer and Buettner, 2001; Marí et al., 2009). Thus, we hypothesized that Sirt3 may regulate the mitochondrial glutathione antioxidant system under CR conditions. To test this hypothesis, we measured the ratio of GSH:GSSG in the mitochondria of the inner ear, brain, and liver of control diet and calorie-restricted WT and *Sirt3*^{-/-} mice at 5 months of age. Mitochondrial GSSG levels decreased during CR in the inner ear from WT mice, but not from *Sirt3*^{-/-} mice (Figure 3B; see also Figure 3C). We also found that the ratios of

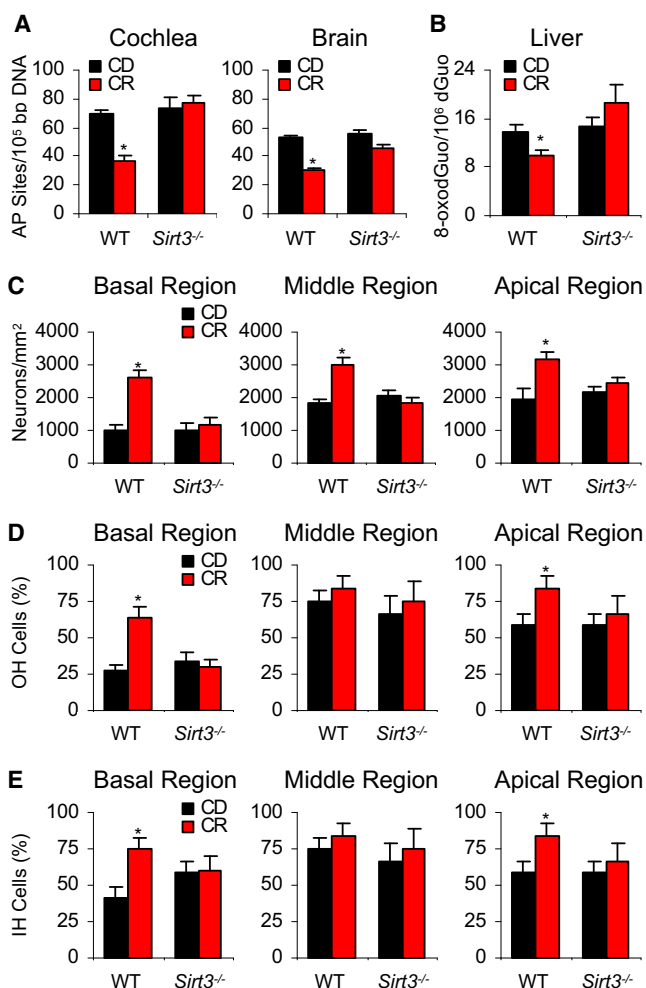


Figure 2. CR Reduces Oxidative DNA Damage and Increases Cell Survival in the Cochlea from WT Mice, but Not from *Sirt3*^{-/-} Mice

(A) Oxidative damage to DNA (apurinic/aprimidinic sites) was measured in the cochlea and neocortex from control diet and calorie-restricted WT and *Sirt3*^{-/-} mice at 12 months of age (n = 4–5). AP sites, apurinic/aprimidinic sites. *Significantly different from 12-month-old WT mice (p < 0.05).

(B) Oxidative damage to DNA (8-oxodGuo) was measured in the liver from control diet and calorie-restricted WT and *Sirt3*^{-/-} mice at 12 months of age (n = 4–5).

(C) Neuron survival (neuron density) of basal, middle, and apical cochlear regions was measured from control diet and calorie-restricted WT and *Sirt3*^{-/-} mice at 12 months of age (n = 4–5).

(D) OH (outer hair) cell survival (%) of basal, middle, and apical cochlear regions was measured from control diet and calorie-restricted WT and *Sirt3*^{-/-} mice at 12 months of age (n = 4–5).

(E) IH (inner hair) cell survival (%) of basal, middle, and apical cochlear regions was measured from control diet and calorie-restricted WT and *Sirt3*^{-/-} mice at 12 months of age (n = 4–5).

Data are means ± SEM. See also Figures 1B–1M.

GSH:GSSG in mitochondria increased during CR in all of the tested WT tissues (Figure 3A); however, CR failed to increase the ratios of GSH:GSSG in *Sirt3*^{-/-} tissues (Figure 3A). These results are consistent with the histological, cochlear cell counting, and oxidative DNA damage results that demonstrated that

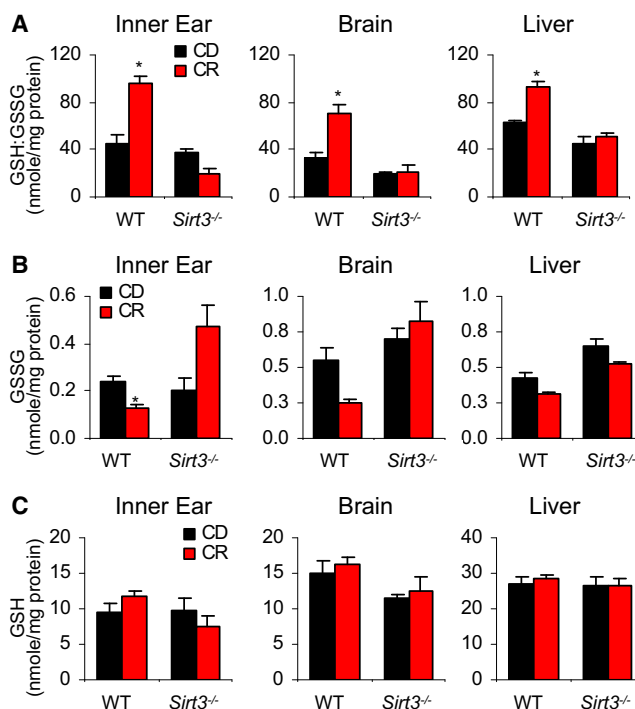


Figure 3. *Sirt3* Increases the Ratios Of GSH:GSSG in Mitochondria during CR

(A–C) Ratios of GSH:GSSG (A), GSSG (B), and GSH (C) were measured in the inner ear, brain (neocortex), and liver from control diet and calorie-restricted WT and *Sirt3*^{-/-} mice at 5 months of age (n = 4–5). *Significantly different from 12- or 5-month-old WT mice (p < 0.05). Data are means ± SEM.

CR reduces oxidative damage in WT tissues, but not in the *Sirt3*^{-/-} tissues. Thus, during CR, *Sirt3* promotes a more reductive environment in mitochondria of multiple tissues, thereby enhancing the glutathione antioxidant defense system.

***Sirt3* Stimulates *Idh2* Activity and Increases NADPH Levels in Mitochondria in Response to CR**

Enzymes of mitochondrial antioxidant pathways require NADPH to perform their reductive functions. NADP⁺-dependent *Idh2* from mitochondria converts NADP⁺ to NADPH, thereby promoting regeneration of GSH by supplying NADPH to glutathione reductase (Jo et al., 2001). A previous in vitro study suggested that *Idh2* might be a target of *Sirt3*, as incubation of *Sirt3* with isocitrate dehydrogenase led to an apparent increase in dehydrogenase activity (Schlicker et al., 2008). Thus, we hypothesized that, in response to CR, the mitochondrial deacetylase *Sirt3* might directly deacetylate and activate *Idh2*, thereby regulating the levels of NADPH and, consequently, the glutathione antioxidant defense system.

To provide initial support for the hypothesis that *Sirt3* regulates *Idh2* activity through deacetylation, we measured the acetylation levels of *Idh2* in the liver mitochondria of WT and *Sirt3*^{-/-} mice fed control and CR diets. In WT tissues, acetylation of *Idh2* was substantial in the control diet fed tissues, but CR induced an 8-fold decrease in acetylation (Figures 4A and 4B). Robust acetylation of *Idh2* was observed in *Sirt3*^{-/-} mice from both

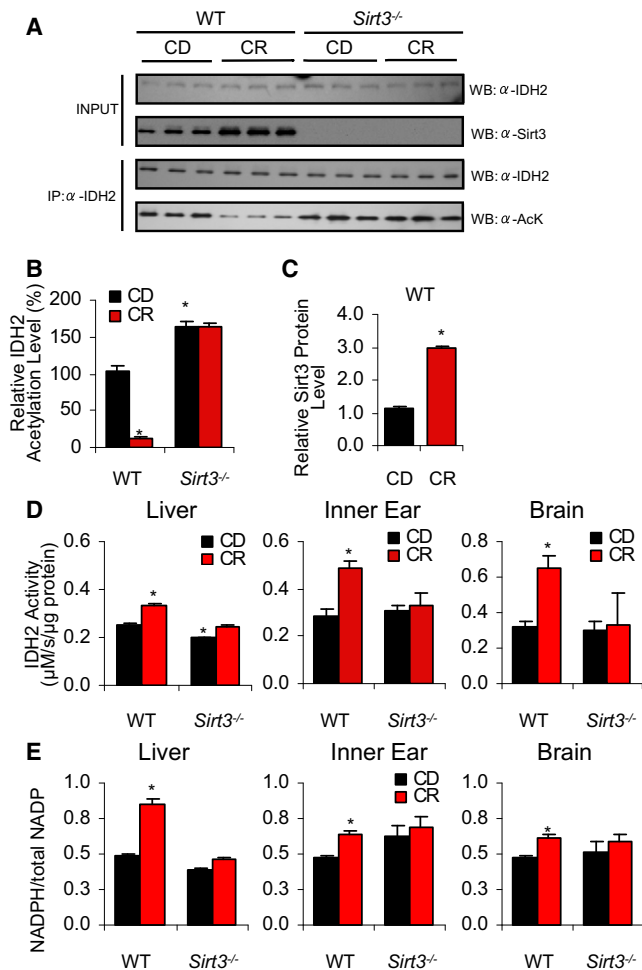


Figure 4. Sirt3 Increases Idh2 Activity and NADPH Levels in Mitochondria by Decreasing the Acetylation State of Idh2 during CR

(A) (Top) Western blot analysis of Sirt3 and Idh2 levels in the liver from 5-month-old WT or *Sirt3*^{-/-} fed either control or calorie-restricted diet. (Bottom) Endogenous acetylated Idh2 was isolated by immunoprecipitation with anti-Idh2 antibody followed by western blotting with anti-acetyl-lysine antibody (n = 3). (B and C) Quantification of the amounts of total Idh2 acetylation (B) and Sirt3 protein (C) from (A). Western blot was normalized with Idh2 levels or Sirt3 levels quantified and analyzed by Image software (n = 3).

(D) Idh2 activities were measured in the liver, inner ear (cochlea), and brain (neocortex) from control diet and calorie-restricted WT and *Sirt3*^{-/-} mice at 5 months of age (n = 3–5).

(E) Ratios of NADPH:total NADP (NADP⁺ + NADPH) were measured in the liver, inner ear, and brain (neocortex) from control diet and caloric restricted WT and *Sirt3*^{-/-} mice at 5 months of age (n = 3–5). *Significantly different from control diet fed WT mice (p < 0.05).

Data are means ± SEM.

control and CR diet-fed conditions, indicating that Sirt3 is required for the CR-induced deacetylation of Idh2 (Figures 4A and 4B). As predicted, CR induced Sirt3 protein levels that were approximately three times higher than those observed with control diet tissues in WT mice (Figure 4C).

To establish whether Idh2 activity is stimulated by Sirt3 under CR conditions, we measured Idh2 activity in the mitochondria

from the liver, inner ear, and brain of control diet and calorie-restricted WT and *Sirt3*^{-/-} mice. We found that Idh2 activity significantly increased during CR in all of the WT tissues (Figure 4D); however, CR failed to increase Idh2 activity in the *Sirt3*^{-/-} tissues (Figure 4D). If CR can induce a Sirt3-dependent increase in Idh2 activity, we anticipated increased levels of NADPH, providing the primary source of reducing equivalents for the glutathione antioxidant system (Jo et al., 2001; Schafer and Buettner, 2001). To test this hypothesis, we measured NADPH levels in mitochondria of WT and *Sirt3*^{-/-} mice. We found that levels of NADPH increased during CR in all tissues tested from WT mice (Figure 4E); however, no significant changes in NADPH levels were observed between control diet and CR *Sirt3*^{-/-} tissues. Collectively, these results provide evidence that, during CR, Sirt3 induces the deacetylation and activation of Idh2, leading to increased levels of NADPH in mitochondria of multiple tissues. We note that we observed a reduction in Idh2 activity in liver from *Sirt3*^{-/-} mice fed the control diet and that this correlates with a slightly increased level of acetylated Idh2 as compared to WT mice (Figure 4B). However, we did not observe reduced Idh2 activity or reduced NADPH levels in the inner ear or brain of *Sirt3*^{-/-} mice. We postulate that, under basal conditions (control diet fed), additional factors regulate mitochondrial Idh2 activity and NADPH levels.

To provide direct evidence that Sirt3 deacetylates Idh2, a number of biochemical experiments were performed. Although most enzyme:substrate reactions are necessarily transient interactions to promote rapid turnover, coimmunoprecipitation (co-IP) experiments can sometimes trap these interactions. Co-IP experiments were performed in human kidney cells (HEK293) cotransfected with Sirt3 and Idh2. We found that precipitated Idh2-FLAG was able to co-IP Sirt3-HA (Figure 5A), whereas precipitated Sirt3-FLAG was able to co-IP Idh2-MYC (Figure 5B), suggesting that a physical interaction can occur between Sirt3 and Idh2 in human cells. However, co-IP experiments do not prove a direct functional interaction. To provide support for a functional interaction between Sirt3 and acetylated Idh2, deacetylation assays were carried out in HEK293 cells (Figure 5C) and in vitro using purified components (Figure 5D). Utilizing HEK293 cells, Idh2 was cotransfected with or without Sirt3, isolated by immunoprecipitation with anti-MYC antibody followed by western blotting with anti-acetyl-lysine antibody. Coexpression with Sirt3 induced the deacetylation of Idh2 to background levels (Figure 5C). For the in vitro analysis, acetylated Idh2 was prepared (see Figure S4 and Experimental Procedures) and utilized as a substrate for purified recombinant Sirt3 or Sirt5. Acetylation status was assessed by western blotting with anti-acetyl-lysine antibody (Figure 5D), and the resulting change in Idh2 activity was measured separately (Figure 5E). We found that Sirt3, but not Sirt5, deacetylated IDH2 in an NAD⁺-dependent fashion (Figure 5E). The corresponding Idh2 activity measurements indicated that deacetylation by Sirt3, but not Sirt5, stimulated Idh2 activity by ~100% (Figure 5E). Together, these data provide strong biochemical evidence that Sirt3 deacetylates and stimulates Idh2 activity and increases NADPH levels in mitochondria in response to CR.

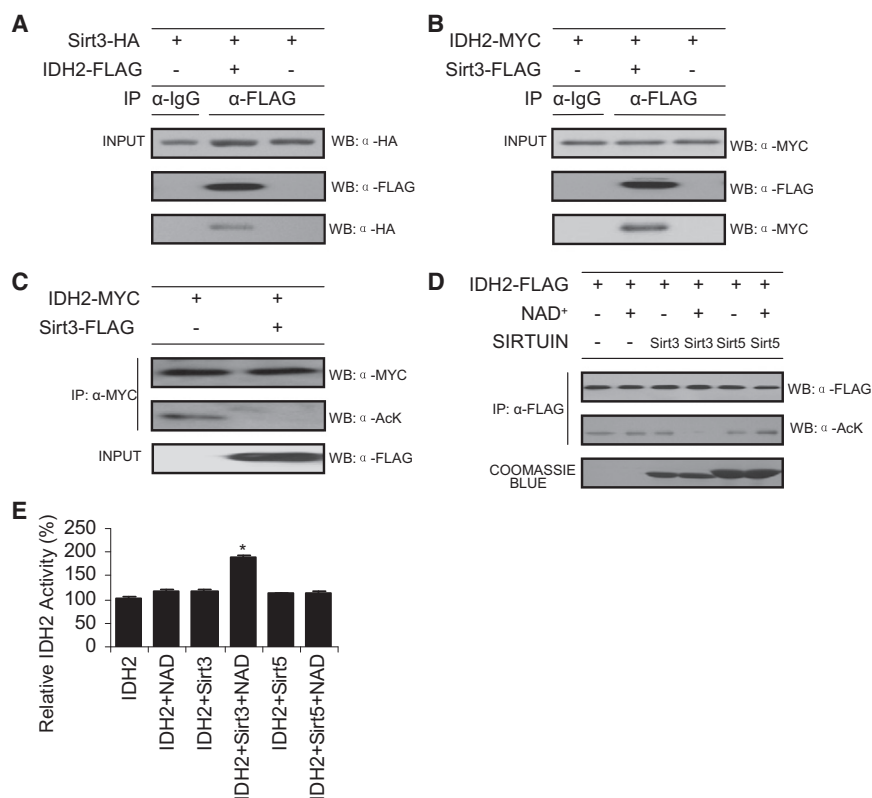


Figure 5. Sirt3 Directly Deacetylates Idh2 and Stimulates Activity

(A and B) Sirt3 interacts with Idh2. Idh2 or Sirt3 were immunoprecipitated from HEK293 cell lysates with IgG antibody or FLAG beads. Precipitated Idh2-FLAG was detected by anti-FLAG antibody, and co-IP Sirt3-HA was detected by anti-HA as indicated (A). Precipitated Sirt3-FLAG was detected by anti-FLAG antibody, and co-IP Idh2-MYC was detected by anti-MYC as indicated (B) (n = 3).

(C) Sirt3 deacetylates Idh2 in HEK293 cells. Idh2 was cotransfected with or without Sirt3, isolated by immunoprecipitation with anti-MYC antibody followed by western blotting with anti-acetyl-lysine antibody (n = 3).

(D) Sirt3, but not Sirt5, deacetylates Idh2 in vitro. Acetylated Idh2 was prepared as outlined in the [Experimental Procedures](#) and was incubated with purified recombinant Sirt3 or Sirt5 with or without NAD⁺ at 37°C for 1 hr. Acetylation status was assessed by western blotting with anti-acetyl-lysine antibody (n = 3). An anti-FLAG western shows that equivalent Idh2 protein levels were used, and Coomassie staining shows purified Sirt3 and Sirt5.

(E) In vitro deacetylation of Idh2 by Sirt3, but not Sirt5, stimulates Idh2 activity. Acetylated Idh2 in buffer (Tris [pH 7.5], with or without 1 mM NAD, and 1 mM DTT) was incubated with purified 50 nM Sirt3 or Sirt5 (Hallows et al., 2006) at 37°C for 1 hr, followed by Idh2 activity assay (n = 3). *Significantly different from Idh2 alone (p < 0.05).

Data are means ± SEM. See also [Figure S4](#).

Overexpression of Sirt3 and/or Idh2 Increases NADPH Levels and Protects Cells from Oxidative Stress-Induced Cell Death

Our physiological, histological, and biochemical results indicate that Sirt3 mediates reduction of oxidative damage by deacetylation and stimulating the activity of Idh2, which increases NADPH levels for antioxidant systems in mitochondria during CR. To provide support for this mechanism, we investigated whether Sirt3 and Idh2 are sufficient to alter the NADPH levels in cultured cells. HEK293 cells stably transfected with vector, Sirt3, Idh2, or Sirt3 with Idh2 were generated, and their NADPH levels were measured. NADPH levels were significantly increased when either Idh2 or Sirt3 or both proteins were stably overexpressed in HEK293 cells ([Figures 6A and 6B](#)). Importantly, overexpression of both Sirt3 and Idh2 yielded a greater increase in NADPH levels than either Sirt3 or Idh2 overexpressed alone ([Figure 6A](#)). Finally, to investigate whether overexpression of Sirt3, Idh2, or Sirt3 with Idh2 can protect cells from oxidative stress, the four HEK293 cell lines were treated with oxidants H₂O₂ (hydrogen peroxide) ([Figure 6C](#)) or menadione ([Figure 6D](#)), and cell viability was measured. Overexpression of Sirt3 or Idh2 was sufficient to protect cells from oxidative stress induced by both oxidants ([Figures 6C and 6D](#)). Again, overexpression of both Sirt3 and Idh2 led to higher cell viability than either Sirt3 or Idh2 overexpressed alone ([Figures 6C and 6D](#)). These results provide strong biochemical evidence that Sirt3 mediates reduction of oxidative

stress by stimulating Idh2 activity and increasing NADPH levels under stress conditions.

DISCUSSION

Sirt3 Reduces Oxidative Damage and Enhances the Glutathione Antioxidant Defense System under CR Conditions

A widely accepted hypothesis of how aging leads to age-related hearing loss is through the accumulation of oxidative damage in the inner ear ([Someya and Prolla, 2010; Liu and Yan, 2007](#)). In support of this hypothesis, oxidative protein damage increases in the cochlea of CBA/J mice ([Jiang et al., 2007](#)), and oxidative DNA damage increases in the cochlea of C57BL/6J mice during aging ([Someya et al., 2009](#)). Age-related hair cell loss is also enhanced in mice lacking the antioxidant enzyme superoxide dismutase 1 ([McFadden et al., 1999](#)), whereas the same mutant animals show enhanced susceptibility to noise-induced hearing loss ([Ohlemiller et al., 1999](#)). We have shown recently that overexpression of mitochondrially targeted catalase delays the onset of AHL in C57BL/6J mice, reduces hair cell loss, and reduces oxidative DNA damage in the inner ear ([Someya et al., 2009](#)). Of interest, overexpression of catalase in the mitochondria leads to extension of life span in C57BL/6J mice, but overexpression of catalase in the peroxisome or nucleus does not ([Schriner et al., 2005](#)). Under normal conditions, catalase decomposes

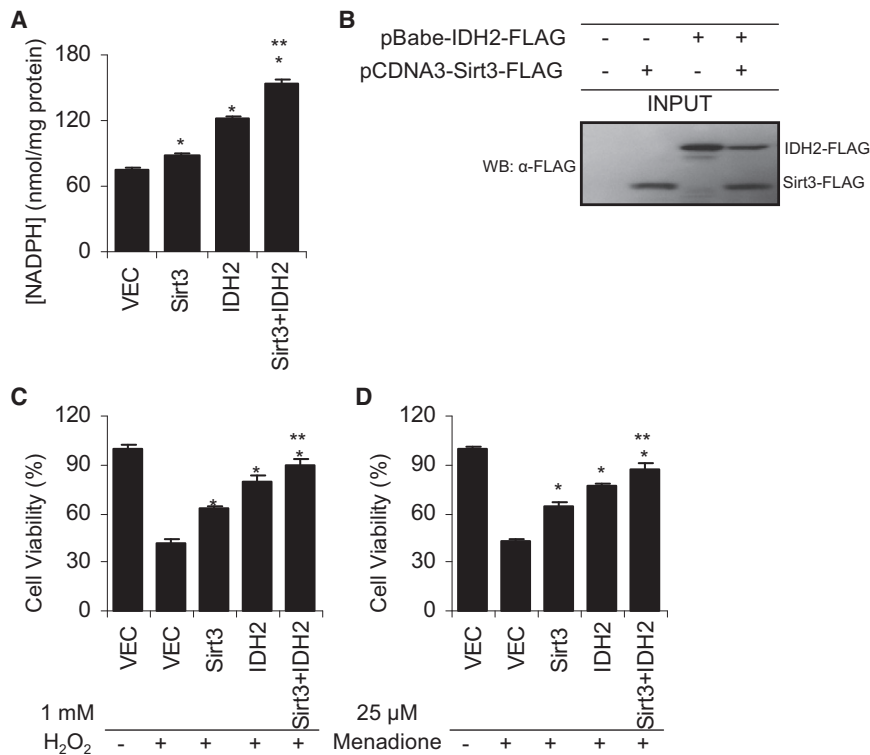


Figure 6. Overexpression of Sirt3 and/or Idh2 Is Sufficient to Increase NADPH Levels and Protects HEK293 Cells from Oxidative Stress

(A and B) (A) NADPH concentrations were significantly increased when either *Idh2* or *Sirt3* or both were stably overexpressed in HEK293 cells. Measurements with errors are shown for the four different stable cell populations from each type of transfection (vector alone, *Sirt3*, *Idh2*, and *Sirt3* with *Idh2*) ($n = 3$). *Significantly different from vector alone ($p < 0.05$); **Significantly different from *Idh2* or *Sirt3* ($p < 0.05$). (B) Western blotting confirms *Idh2* and *Sirt3* stable expression. (C and D) *Sirt3* and/or *Idh2* overexpression is sufficient to protect HEK293 cells from the exogenous oxidants hydrogen peroxide (H_2O_2) (C) and menadione (D). The four different stable cells were transiently exposed to either 1 mM H_2O_2 or 25 μM menadione ($n = 16$). Data are means \pm SEM.

hydrogen peroxide in the peroxisome, whereas in mitochondria, hydrogen peroxide is decomposed into water by glutathione peroxidase or peroxiredoxin (Finkel and Holbrook, 2000; Mari et al., 2009). Hence, these results suggest that mitochondrial ROS play a critical role in cochlear aging, AHL, and aging in general.

We have demonstrated that *Sirt3* mediates the CR reduction of oxidative DNA damage in multiple tissues and that these effects are likely to arise through an enhanced mitochondrial glutathione antioxidant defense system. As discussed earlier, the GSH:GSSG ratio is thought to be a marker of oxidative stress (Rebrin and Sohal, 2008). Experimental evidence indicates that aging results in a decrease in the ratio of GSH:GSSG in the mitochondria of brain, liver, kidney, eye, heart, and testis from aged C57BL/6J mice due to elevated levels of GSSG, whereas CR decreases the ratio of GSH:GSSG in the mitochondria of these tissues by lowering GSSG levels (Rebrin et al., 2003, 2007). Our findings demonstrate that CR increases these ratios of GSH:GSSG in the mitochondria of brain, liver, and inner ear from WT mice but fails to increase the ratios in the same tissues from *Sirt3*^{-/-} mice. Consistent with these results, CR reduced oxidative DNA damage in tissues from WT mice but failed to reduce such damage in tissues from *Sirt3*^{-/-} mice. CR also increased spiral ganglion neuron and hair cell survival in the WT cochlea, but not in *Sirt3*^{-/-} mice. Tissues that are composed of postmitotic cells such as the brain and the inner ear are particularly vulnerable to oxidative damage because of their high energy requirements and inability to undergo regeneration. Therefore, we speculate that the *Sirt3*-mediated modulation of

the glutathione antioxidant defense system may play a central role in reduction of oxidative stress in multiple tissues under CR conditions, leading to aging retardation. We also note that other mitochondrial effects of *Sirt3*, such as regulation of fatty acid oxidation (Hirschey et al., 2010) and modulation of complex I activity (Ahn, et al., 2008), are likely to contribute to the metabolic adaptations in response to CR.

Idh2 Regulates the Redox State of Mitochondria under CR Conditions

A large body of evidence indicates that the antioxidant defense systems do not keep pace with the age-related increase in ROS production, and thus the balance between antioxidant defenses and ROS production shifts progressively toward a more pro-oxidant state during aging (Sohal and Weindruch, 1996; Rebrin and Sohal, 2008). This balance is determined in part by the ratios of interconvertible forms of redox couples, such as GSH/GSSG, NADPH/NADP⁺, NADH/NAD⁺, thioredoxin_{red}/thioredoxin_{oxid}, and glutaredoxin_{red}/glutaredoxin_{oxid}. The GSH/GSSG couple is thought to be the primary cellular determinant of the cellular redox state because its abundance is three to four orders of magnitude higher than the other redox couples (Rebrin and Sohal, 2008). NADPH is the reducing equivalent required for the regeneration of GSH and the GSH-mediated antioxidant defense system, which includes glutathione peroxidases, glutathione transferases, and glutathione reductase, playing a critical role in oxidative stress resistance (Halliwell and Gutteridge, 2007). GSH is synthesized in the cytosol and transported into the mitochondria through protein channels in the outer mitochondrial membrane (Halliwell and Gutteridge, 2007; Anderson, 1998). Although GSH can cross the outer mitochondrial membrane through these channels, GSSG cannot be exported into the cytosol (Olafsdottir and Reed, 1988). Thus, GSSG is reduced to GSH by mitochondrial NADPH-dependent

glutathione reductase, preventing accumulation of GSSG in the mitochondrial matrix (Schafer and Buettner, 2001; Mari et al., 2009). We have demonstrated that Sirt3 directly deacetylates and activates Idh2 under CR conditions. In response to CR, deacetylated Idh2 displays increased catalytic activity, which is correlated with increased NADPH levels in the mitochondria of multiple tissues from WT mice, but not from *Sirt3*^{-/-} mice. Hence, we speculate that Idh2 may be a major player in regulating the redox state of mitochondria under CR conditions given its role in mitochondrial NADPH production. A previous study has shown that Idh2 is induced in response to ROS in mouse fibroblasts, whereas decreased levels of Idh2 lead to higher ROS and accumulation of oxidative damage to DNA and lipids (Jo et al., 2001). Our in vitro findings demonstrate that overexpression of Sirt3 and/or Idh2 increases NADPH levels and protects cells from oxidative stress-induced cell death. Thus, these observations underlie a critical role for Idh2 in the generation of NADPH in mitochondria under conditions of CR, providing reducing capacity for the glutathione antioxidant system and increasing oxidative stress resistance.

A Role for Sirt3 in CR-Mediated Prevention of AHL

The mouse is considered a good model for the study of human AHL because the mouse cochlea is anatomically similar to that of humans (Steel et al., 1996; Steel and Bock, 1983). Most inbred mouse strains display some degree of AHL, and the age of onset of AHL is known to vary from 3 months in DBA/2J mice to more than 20 months in CBA/CaJ mice (Zheng et al., 1999). The C57BL/6J mouse strain, which is the most widely used mouse model for the study of aging, displays the classic pattern of AHL by 12–15 months of age (Hunter and Willott, 1987; Keithley et al., 2004). We have previously shown that AHL in C57BL/6J mice occurs through Bak-mediated apoptosis and that it can be prevented by the intake of small molecule antioxidants (Someya et al., 2009). We note that C57BL/6J and many other mouse strains carry a specific mutation (*Cdh23*^{753A}) in the *Cdh23* gene, which encodes a component of the hair cell tip link, and this mutation is known to promote early onset of AHL in these animals (Noben-Trauth et al., 2003). Of interest, the *Cdh23*^{753A} allele may increase the susceptibility to oxidative stress in hair cells because a *Sod1* mutation greatly enhances AHL in mice carrying *Cdh23*^{753A}, but not in mice wild-type for *Cdh23* (Johnson, et al., 2010). However, oxidative damage increases with age in the cochlea of both C57BL/6J mice and the CBA/J mouse strain that does not carry the *Cdh23*^{753A} allele, indicating that oxidative stress plays a role in AHL independent of *Cdh23* (Someya et al., 2009; Jiang et al., 2007; Zheng et al., 1999). In both strains, the loss of hair cells and spiral ganglion neurons begins in the base of the cochlea and spreads toward the apex with age (Keithley et al., 2004; Hunter and Willott, 1987). Importantly, CR slows the progression of AHL in both C57BL/6J and CBA/J strains (Someya et al., 2007; Sweet et al., 1988). Therefore, the protective effects of Sirt3 in AHL are likely to be of general relevance to AHL.

It is thought that some of the effects of CR in aging retardation require significant reduction of body weight through reducing food consumption. In agreement with this hypothesis, obesity promotes a variety of age-related diseases, such as cardiovas-

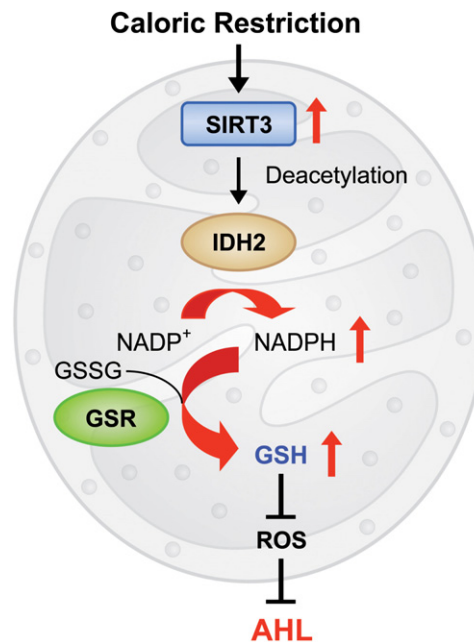


Figure 7. A Model for the CR-Mediated Prevention of AHL in Mammals

In response to CR, SIRT3 activates IDH2, thereby increasing NADPH levels in mitochondria. This in turn leads to an increased ratio of GSH:GSSG and decreased levels of ROS, thereby resulting in protection from oxidative stress and prevention of AHL in mammals.

cular disease, diabetes, high blood pressure, hypertension, and certain cancers (Paeratakul et al., 2002; Poirier et al., 2006). Obesity is also associated with an increased risk of mortality (Poirier et al., 2006; Lee et al., 1993). Of interest, CR failed to reduce oxidative damage in multiple tissues and slow the progression of AHL in CR *Sirt3*^{-/-} mice, despite the fact that these mice were lean (Figures S2A and S2B). Thus, these results suggest that weight loss may not be sufficient for the anti-aging action of CR. Instead, we postulate that critical metabolic effectors such as Sirt3 mediate the positive effects of CR.

Conclusions

In summary, we propose that, in response to CR, Sirt3 activates Idh2, thereby increasing NADPH levels in mitochondria. This in turn leads to increased ratios of GSH:GSSG in mitochondria and decreased levels of ROS, resulting in protection of inner ear cells and prevention of AHL in mammals (Figure 7). Because we observed similar effects of CR in the mitochondrial GSH/GSSG ratios in multiple tissues, we postulate that this may be a major mechanism of aging retardation by CR. We also postulate that pharmaceutical interventions that induce Sirt3 activity in multiple tissues will mimic CR by increasing oxidative stress resistance and preventing the mitochondrial decay associated with aging.

EXPERIMENTAL PROCEDURES

Animals

Male and female *Sirt3*^{-/-} mice were purchased from the Mutant Mouse Resource Centers (MMRRC) at the University of North Carolina-Chapel Hill

(Chapel Hill, NC). In brief, these mice were created by generating embryonic stem (ES) cells (Omni bank number OST341297) bearing a retroviral promoter trap that functionally inactivates one allele of the *Sirt3* gene (MGI, 2010). Male and female C57BL/6J mice were purchased from Jackson Laboratory (Bar Harbor, ME). *Sirt3*^{+/-} mice have been backcrossed for four generations onto the C57BL/6J background. All animal studies were conducted at the AAALAC-approved Animal Facility in the Genetics and Biotechnology Center of the University of Wisconsin-Madison. Experiments were performed in accordance with protocols approved by the University of Wisconsin-Madison Institutional Animal Care and Use Committee (Madison, WI).

Dietary Study

Details on the methods used to house and feed mice have been described previously (Pugh et al., 1999). Mice are housed individually. Control diet (CD) groups were fed 86.4 kcal/week of the precision pellet diet AIN-93M (BioServ, Frenchtown, NJ), and caloric-restricted (CR) groups were fed 64.8 kcal/week (a 25% CR) of the precision pellet diet AIN-93M 40%DR (BioServ, Frenchtown, NJ). The schedule of feeding for control diet was 7 g on Mondays and Wednesdays and 10 g on Fridays, whereas the schedule of feeding for caloric-restricted diets was 5 g on Mondays and Wednesdays and 8 g on Fridays. This dietary regimen was maintained from 2 months of age until 5 months of age for a 3 month CR study and from 2 months of age until 12 months of age for a 10 month CR study.

ABR Hearing Test

At 12 months of age, ABRs were measured with a tone burst stimulus at 8, 16, and 32 kHz using an ABR recording system (Intelligent Hearing System, Miami, FL) as previously described (Someya et al., 2009). Mice were anesthetized with a mixture of xylazine hydrochloride (10 mg/kg, i.m.) (Phoenix Urology of St. Joseph, St. Joseph, MO) and ketamine hydrochloride (40 mg/kg, i.m.) (Phoenix Urology of St. Joseph).

Measurement of DNA Oxidation Levels

At 12 months of age, cochlea and neocortex were collected, and DNA was extracted with ethanol precipitation. DNA concentrations for each sample were adjusted to 0.1 μg/ml, and numbers of apurinic/aprimidinic (AP) sites were determined using the DNA Damage Quantification Kit (Dojindo, Rockville, MD) and performed according to the manufacturer's instructions and as previously described (Kubo et al., 1992; Meira, et al., 2009; McNeill and Wilson, 2007). Liver was also collected from the same mice, and 8-hydroxyguanosine levels (8-oxo-7,8-2'-deoxyguanosine/10⁶ deoxyguanosine) in the DNA were determined using a HPLC-ECD method as previously described (Hofer et al., 2006).

Measurement of Total GSH and GSSG

Just after mitochondrial lysate preparation, 100 μl of the lysate was mixed with 100 μl of 10% metaphosphoric acid, incubated for 30 min at 4°C, and centrifuged at 14,000 × g for 10 min at 4°C. The supernatant was used for the measurements of mitochondrial glutathione contents. Total glutathione (GSH + GSSG) and GSSG levels were determined by the method of Rahman et al. (2006). All samples were run in duplicate. The rates of 2-nitro-5-thiobenzoic acid formation were calculated, and the total glutathione (tGSH) and GSSG concentrations in the samples were determined by using linear regression to calculate the values obtained from the standard curve. The GSH concentration was determined by subtracting the GSSG concentration from the tGSH concentration.

Idh2 Acetylation Analysis

Antibodies used for western blotting included anti-Idh2 antibody (Santa Cruz, Santa Cruz, CA), anti-Sirt3 antibody (gift of Dr. Eric Verdin, UCSF), protein A/G plus agarose (Santa Cruz, Santa Cruz, CA), and pan-acetylated lysine (generated following the procedure of Zhao, et al. [2010], GeneTel Laboratories LLC, Madison, WI). For immunoprecipitation, liver mitochondria lysates were incubated with anti-Idh2 antibody overnight at 4°C. Then protein A/G plus agarose were added and incubated for 3 hr. After resins were washed, samples were boiled with SDS loading buffer and subjected to western blotting (Smith et al., 2009).

Idh2 Activity

Activities of Idh2 were measured by the Kornberg method (Kornberg, 1955). In brief, 20 μl of the mitochondrial lysate sample was added in each well of a 96-well plate, and then 180 μl of a reaction mixture (33 mM KH₂PO₄•K₂HPO₄, 3.3 mM MgCl₂, 167 μM NADP⁺, and 167 μM (+)-potassium Ds-threo-isocitrate monobasic) was added in each well. The absorbance was immediately read at 340 nm every 10 s for 1 min in a microplate reader (Bio-Rad, Hercules, CA). All samples were run in duplicate. The reaction rates were calculated, and the Idh2 activity in the sample was defined as the production of one μmole of NADPH per sec.

In Vitro Deacetylation Assay

Idh2-FLAG was transfected into HEK293 cells, which were then treated with 5 mM nicotinamide for 16 hr. Nicotinamide is a widely used sirtuin inhibitor. Nicotinamide treatment leads to increased acetylation of Idh2, with a corresponding decrease in enzymatic activity (Figure S4). Idh2 from cell lysates was immunoprecipitated with anti-FLAG beads at 4°C for 2 hr, and then Idh2-FLAG on beads was utilized in 200 μl deacetylation buffer (Tris [pH 7.5], with or without 1 mM NAD, and 1 mM DTT) and incubated with purified 50 nM Sirt3 or Sirt5 (Hallows et al., 2006) at 37°C for 1 hr. Aliquots were removed for Idh2 activity assay and western blotting with anti-FLAG antibody or anti-acetyl-lysine antibody.

Statistical Analysis

All Statistical analyses were carried out by one-way ANOVA with post-Tukey multiple comparison tests using the Prism 4.0 statistical analysis program (GraphPad, San Diego, CA). All tests were two-sided with statistical significance set at p < 0.05.

SUPPLEMENTAL INFORMATION

Supplemental Information includes Extended Experimental Procedures, four figures, and one table and can be found at doi:10.1016/j.cell.2010.10.002.

ACKNOWLEDGMENTS

We thank S. Kinoshita for histological processing. This research was supported by NIH grants AG021905 (T.A.P.) and GM065386 (J.M.D.), the National Projects on Protein Structural and Functional Analyses from the Ministry of Education, Culture, Sports, Science, and Technologies of Japan, and Marine Bio Foundation.

Received: July 19, 2010

Revised: September 3, 2010

Accepted: September 30, 2010

Published online: November 18, 2010

REFERENCES

- Ahn, B.H., Kim, H.S., Song, S., Lee, I.H., Liu, J., Vassilopoulos, A., Deng, C.X., and Finkel, T. (2008). A role for the mitochondrial deacetylase Sirt3 in regulating energy homeostasis. *Proc. Natl. Acad. Sci. USA* 105, 14447–14452.
- Anderson, M.E. (1998). Glutathione: an overview of biosynthesis and modulation. *Chem. Biol. Interact.* 111–112, 1–14.
- Balaban, R.S., Nemoto, S., and Finkel, T. (2005). Mitochondria, oxidants, and aging. *Cell* 120, 483–495.
- Barger, J.L., Kayo, T., Vann, J.M., Arias, E.B., Wang, J., Hacker, T.A., Wang, Y., Raederstorff, D., Morrow, J.D., Leeuwenburgh, C., et al. (2008). A low dose of dietary resveratrol partially mimics caloric restriction and retards aging parameters in mice. *PLoS ONE* 3, e2264.
- Bordone, L., Cohen, D., Robinson, A., Motta, M.C., van Veen, E., Czopik, A., Steele, A.D., Crowe, H., Marmor, S., Luo, J., et al. (2007). SIRT1 transgenic mice show phenotypes resembling caloric restriction. *Aging Cell* 6, 759–767.
- Chen, D., Steele, A.D., Lindquist, S., and Guarente, L. (2005). Increase in activity during caloric restriction requires Sirt1. *Science* 310, 1641.

- Chen, D., Bruno, J., Easlon, E., Lin, S.J., Cheng, H.L., Alt, F.W., and Guarente, L. (2008). Tissue-specific regulation of SIRT1 by calorie restriction. *Genes Dev.* 22, 1753–1757.
- Cohen, H.Y., Miller, C., Bitterman, K.J., Wall, N.R., Hekking, B., Kessler, B., Howitz, K.T., Gorospe, M., de Cabo, R., and Sinclair, D.A. (2004). Calorie restriction promotes mammalian cell survival by inducing the SIRT1 deacetylase. *Science* 305, 390–392.
- Colman, R.J., Anderson, R.M., Johnson, S.C., Kastman, E.K., Kosmatka, K.J., Beasley, T.M., Allison, D.B., Cruzen, C., Simmons, H.A., Kemnitz, J.W., and Weindruch, R. (2009). Caloric restriction delays disease onset and mortality in rhesus monkeys. *Science* 325, 201–204.
- Donmez, G., and Guarente, L. (2010). Aging and disease: connections to sirtuins. *Aging Cell* 9, 285–290.
- Finkel, T., and Holbrook, N.J. (2000). Oxidants, oxidative stress and the biology of ageing. *Nature* 408, 239–247.
- Finkel, T., Deng, C.X., and Mostoslavsky, R. (2009). Recent progress in the biology and physiology of sirtuins. *Nature* 460, 587–591.
- Halliwell, B., and Gutteridge, J.M.C. (2007). *Free Radicals in Biology and Medicine* (New York, NY: Oxford University Press).
- Hallows, W.C., Lee, S., and Denu, J.M. (2006). Sirtuins deacetylate and activate mammalian acetyl-CoA synthetases. *Proc. Natl. Acad. Sci. USA* 103, 10230–10235.
- Hamilton, M.L., Van Remmen, H., Drake, J.A., Yang, H., Guo, Z.M., Kewitt, K., Walter, C.A., and Richardson, A. (2001). Does oxidative damage to DNA increase with age? *Proc. Natl. Acad. Sci. USA* 98, 10469–10474.
- Hirschey, M.D., Shimazu, T., Goetzman, E., Jing, E., Schwer, B., Lombard, D.B., Grueter, C.A., Harris, C., Biddinger, S., Ikkayeva, O.R., et al. (2010). SIRT3 regulates mitochondrial fatty-acid oxidation by reversible enzyme deacetylation. *Nature* 464, 121–125.
- Hofer, T., Seo, A.Y., Prudencio, M., and Leeuwenburgh, C. (2006). A method to determine RNA and DNA oxidation simultaneously by HPLC-ECD: greater RNA than DNA oxidation in rat liver after doxorubicin administration. *Biol. Chem.* 387, 103–111.
- Hunter, K.P., and Willott, J.F. (1987). Aging and the auditory brainstem response in mice with severe or minimal presbycusis. *Hear. Res.* 30, 207–218.
- Jiang, H., Talaska, A.E., Schacht, J., and Sha, S.H. (2007). Oxidative imbalance in the aging inner ear. *Neurobiol. Aging* 28, 1605–1612.
- Jo, S.H., Son, M.K., Koh, H.J., Lee, S.M., Song, I.H., Kim, Y.O., Lee, Y.S., Jeong, K.S., Kim, W.B., Park, J.W., et al. (2001). Control of mitochondrial redox balance and cellular defense against oxidative damage by mitochondrial NADP⁺-dependent isocitrate dehydrogenase. *J. Biol. Chem.* 276, 16168–16176.
- Johnson, K.R., Yu, H., Ding, D., Jiang, H., Gagnon, L.H., and Salvi, R.J. (2010). Separate and combined effects of Sod1 and Cdh23 mutations on age-related hearing loss and cochlear pathology in C57BL/6J mice. *Hear. Res.* 268, 85–92.
- Keithley, E.M., Canto, C., Zheng, Q.Y., Fischel-Ghodsian, N., and Johnson, K.R. (2004). Age-related hearing loss and the ahl locus in mice. *Hear. Res.* 188, 21–28.
- Kornberg, A. (1955). Isocitric dehydrogenase of yeast (TPN). *Methods Enzymol.* 1, 705–707.
- Koubova, J., and Guarente, L. (2003). How does calorie restriction work? *Genes Dev.* 17, 313–321.
- Kubo, K., Ide, H., Wallace, S.S., and Kow, Y.W. (1992). A novel, sensitive, and specific assay for abasic sites, the most commonly produced DNA lesion. *Biochemistry* 31, 3703–3708.
- Lee, I.M., Manson, J.E., Hennekens, C.H., and Paffenbarger, R.S., Jr. (1993). Body weight and mortality. A 27-year follow-up of middle-aged men. *JAMA* 270, 2823–2828.
- Lin, S.J., Defossez, P.A., and Guarente, L. (2000). Requirement of NAD and SIR2 for life-span extension by calorie restriction in *Saccharomyces cerevisiae*. *Science* 289, 2126–2128.
- Liu, X.Z., and Yan, D. (2007). Ageing and hearing loss. *J. Pathol.* 211, 188–197.
- Marí, M., Morales, A., Colell, A., García-Ruiz, C., and Fernández-Checa, J.C. (2009). Mitochondrial glutathione, a key survival antioxidant. *Antioxid. Redox Signal.* 11, 2685–2700.
- Masoro, E.J. (2000). Caloric restriction and aging: an update. *Exp. Gerontol.* 35, 299–305.
- Mattson, M.P. (2000). Apoptosis in neurodegenerative disorders. *Nat. Rev. Mol. Cell Biol.* 1, 120–129.
- McFadden, S.L., Ding, D., Reaume, A.G., Flood, D.G., and Salvi, R.J. (1999). Age-related cochlear hair cell loss is enhanced in mice lacking copper/zinc superoxide dismutase. *Neurobiol. Aging* 20, 1–8.
- McNeill, D.R., and Wilson, D.M.I.I., III. (2007). A dominant-negative form of the major human abasic endonuclease enhances cellular sensitivity to laboratory and clinical DNA-damaging agents. *Mol. Cancer Res.* 5, 61–70.
- Meira, L.B., Moroski-Erkul, C.A., Green, S.L., Calvo, J.A., Bronson, R.T., Shah, D., and Samson, L.D. (2009). Aag-initiated base excision repair drives alkylation-induced retinal degeneration in mice. *Proc. Natl. Acad. Sci. USA* 106, 888–893.
- MGI. Sirt3^{Gt(OST341297)Lex}. (2010). Available at http://www.informatics.jax.org/searches/accession_report.cgi?id=MGI:3529767.
- Noben-Trauth, K., Zheng, Q.Y., and Johnson, K.R. (2003). Association of cadherin 23 with polygenic inheritance and genetic modification of sensorineural hearing loss. *Nat. Genet.* 35, 21–23.
- Ohlemiller, K.K., McFadden, S.L., Ding, D.L., Flood, D.G., Reaume, A.G., Hoffman, E.K., Scott, R.W., Wright, J.S., Putcha, G.V., and Salvi, R.J. (1999). Targeted deletion of the cytosolic Cu/Zn-superoxide dismutase gene (Sod1) increases susceptibility to noise-induced hearing loss. *Audiol. Neurootol.* 4, 237–246.
- Olafsdottir, K., and Reed, D.J. (1988). Retention of oxidized glutathione by isolated rat liver mitochondria during hydroperoxide treatment. *Biochim. Biophys. Acta* 964, 377–382.
- Paeratakul, S., Lovejoy, J.C., Ryan, D.H., and Bray, G.A. (2002). The relation of gender, race and socioeconomic status to obesity and obesity comorbidities in a sample of US adults. *Int. J. Obes. Relat. Metab. Disord.* 26, 1205–1210.
- Poirier, P., Giles, T.D., Bray, G.A., Hong, Y., Stern, J.S., Pi-Sunyer, F.X., and Eckel, R.H. (2006). Obesity and cardiovascular disease: pathophysiology, evaluation, and effect of weight loss. *Arterioscler. Thromb. Vasc. Biol.* 26, 968–976.
- Pugh, T.D., Klopp, R.G., and Weindruch, R. (1999). Controlling caloric consumption: protocols for rodents and rhesus monkeys. *Neurobiol. Aging* 20, 157–165.
- Rahman, I., Kode, A., and Biswas, S.K. (2006). Assay for quantitative determination of glutathione and glutathione disulfide levels using enzymatic recycling method. *Nat. Protoc.* 1, 3159–3165.
- Rebrin, I., and Sohal, R.S. (2008). Pro-oxidant shift in glutathione redox state during aging. *Adv. Drug Deliv. Rev.* 60, 1545–1552.
- Rebrin, I., Kamzalov, S., and Sohal, R.S. (2003). Effects of age and caloric restriction on glutathione redox state in mice. *Free Radic. Biol. Med.* 35, 626–635.
- Rebrin, I., Forster, M.J., and Sohal, R.S. (2007). Effects of age and caloric intake on glutathione redox state in different brain regions of C57BL/6 and DBA/2 mice. *Brain Res.* 1127, 10–18.
- Schafer, F.Q., and Buettner, G.R. (2001). Redox environment of the cell as viewed through the redox state of the glutathione disulfide/glutathione couple. *Free Radic. Biol. Med.* 30, 1191–1212.
- Schlicker, C., Gertz, M., Papatheodorou, P., Kachholz, B., Becker, C.F., and Steegborn, C. (2008). Substrates and regulation mechanisms for the human mitochondrial sirtuins Sirt3 and Sirt5. *J. Mol. Biol.* 382, 790–801.
- Schriner, S.E., Linford, N.J., Martin, G.M., Treuting, P., Ogburn, C.E., Emond, M., Coskun, P.E., Ladiges, W., Wolf, N., Van Remmen, H., et al. (2005). Extension of murine life span by overexpression of catalase targeted to mitochondria. *Science* 308, 1909–1911.

- Schwer, B., Eckersdorff, M., Li, Y., Silva, J.C., Fermin, D., Kurtev, M.V., Gialourakis, C., Comb, M.J., Alt, F.W., and Lombard, D.B. (2009). Calorie restriction alters mitochondrial protein acetylation. *Aging Cell* 8, 604–606.
- Smith, B.C., Hallows, W.C., and Denu, J.M. (2009). A continuous microplate assay for sirtuins and nicotinamide-producing enzymes. *Anal. Biochem.* 394, 101–109.
- Sohal, R.S., and Weindruch, R. (1996). Oxidative stress, caloric restriction, and aging. *Science* 273, 59–63.
- Someya, S., Yamasoba, T., Weindruch, R., Prolla, T.A., and Tanokura, M. (2007). Caloric restriction suppresses apoptotic cell death in the mammalian cochlea and leads to prevention of presbycusis. *Neurobiol. Aging* 28, 1613–1622.
- Someya, S., Xu, J., Kondo, K., Ding, D., Salvi, R.J., Yamasoba, T., Rabinovitch, P.S., Weindruch, R., Leeuwenburgh, C., Tanokura, M., and Prolla, T.A. (2009). Age-related hearing loss in C57BL/6J mice is mediated by Bak-dependent mitochondrial apoptosis. *Proc. Natl. Acad. Sci. USA* 106, 19432–19437.
- Someya, S., and Prolla, T.A. (2010). Mitochondrial oxidative damage and apoptosis in age-related hearing loss. *Mech. Ageing Dev.* 131, 480–486.
- Steel, K.P., and Bock, G.R. (1983). Hereditary inner-ear abnormalities in animals. Relationships with human abnormalities. *Arch. Otolaryngol.* 109, 22–29.
- Steel, K.P., Moorjani, P., and Bock, G.R. (1996). Mixed conductive and sensorineural hearing loss in LP/J mice. *Hear. Res.* 28, 227–236.
- Sundaresan, N.R., Samant, S.A., Pillai, V.B., Rajamohan, S.B., and Gupta, M.P. (2008). SIRT3 is a stress-responsive deacetylase in cardiomyocytes that protects cells from stress-mediated cell death by deacetylation of Ku70. *Mol. Cell. Biol.* 28, 6384–6401.
- Sundaresan, N.R., Gupta, M., Kim, G., Rajamohan, S.B., Isbatan, A., and Gupta, M.P. (2009). Sirt3 blocks the cardiac hypertrophic response by augmenting Foxo3a-dependent antioxidant defense mechanisms in mice. *J. Clin. Invest.* 119, 2758–2771.
- Sweet, R.J., Price, J.M., and Henry, K.R. (1988). Dietary restriction and presbycusis: periods of restriction and auditory threshold losses in the CBA/J mouse. *Audiology* 27, 305–312.
- Wallace, D.C. (2005). A mitochondrial paradigm of metabolic and degenerative diseases, aging, and cancer: a dawn for evolutionary medicine. *Annu. Rev. Genet.* 39, 359–407.
- Weindruch, R., and Walford, R.L. (1988). *The Retardation of Aging and Disease by Dietary Restriction* (Springfield, IL: Charles C Thomas Publishing, LTD).
- Zhao, S., Xu, W., Jiang, W., Yu, W., Lin, Y., Zhang, T., Yao, J., Zhou, L., Zeng, Y., Li, H., et al. (2010). Regulation of cellular metabolism by protein lysine acetylation. *Science* 327, 1000–1004.
- Zheng, Q.Y., Johnson, K.R., and Erway, L.C. (1999). Assessment of hearing in 80 inbred strains of mice by ABR threshold analyses. *Hear. Res.* 130, 94–107.
- Zhu, H., Guo, Q., and Mattson, M.P. (1999). Dietary restriction protects hippocampal neurons against the death-promoting action of a presenilin-1 mutation. *Brain Res.* 842, 224–229.

EXTENDED EXPERIMENTAL PROCEDURES

Reagents

All chemicals were purchased from Sigma-Aldrich Corp. (St. Louis, MO), unless otherwise indicated.

Genotyping of *Sirt3*^{-/-} Mice

Sirt3^{+/-} males were mated with *Sirt3*^{+/-} females, and the offspring from these mating were genotyped from DNA obtained by a tail clip at weaning. The following primers were used for genotyping: WT forward 5'-ATCTCGCAGATAGGCTATCAGC-3'; WT reverse 5'-AACACGTAACCTTACCCAAGG-3'; KO forward 5'-ATCTCGCAGATAGGCTATCAGC-3'; and KO reverse 5'-ATAAACCTCTTG CAGTTGCATC-3'. The PCR cycling parameters were as follows: 94°C for 5 min; 10 cycles of 94°C for 30 s, 65°C for 30 s (Decrease 1°C/cycle), 72°C for 40 s; and 30 cycles of 94°C for 30 s, 55°C for 30 s, 72°C for 40 s. PCR products were separated on 1.5% agarose gel and the expected band size for WT and *Sirt3*^{-/-} mice were 336 and 160 bps, respectively.

Body Weight

The body weight of the mice was measured every month from 2 months of age until 12 months of age.

Tissue Weight

The tissue weight of the mice was measured at 5 months of age.

Bone Mineral Density and Total Body Fat Percentage

Mice at 5 months of age were anesthetized with 240 mg/kg tribromoethanol, secured to a lightly adhesive tray, and subjected to X-ray densitometry using a PIXImus densitometer (GE Lunar, Madison WI). Bone mineral density (BMD) (femur) and total body fat percentage were calculated using PIXImus software version 1.45.

Serum Glucose Measurement

Mice at 5 months of age were subjected to overnight fasting. Blood samples were then collected from the tail vein the following day. Serum glucose levels were measured using OneTouch Ultra (LifeScan, Milpitas, CA).

Glucose Tolerance Test

Mice at 5 months of age were subjected to overnight fasting followed by intraperitoneal glucose injection (1 g/kg body weight of mice using a solution of 10% glucose in PBS). Blood samples were collected from the tail vein at 0, 30, 60, and 120 min after glucose injection. Serum glucose levels were measured using OneTouch Ultra (LifeScan, Milpitas, CA).

Insulin, Triglycerides, Igh-1, and Cholesterol

Mice at 5 months of age were subjected to overnight fasting. The animals were sacrificed by rapid cervical dislocation and whole blood samples were collected from the axillary artery and vein by incision. Serum insulin and Igh-1 levels were measured by Millipore (Billerica, MA), while serum triglycerides and cholesterol levels were measured by Marshfield Labs (Marshfield, WI).

Cochlear Histology

Following the ABR hearing measurements, the animals were sacrificed by cervical dislocation and the temporal bone was excised from the head and divided into cochlear and vestibular parts (Someya et al., 2009). The cochlea was then excised, immersed in a fixative containing 4% paraformaldehyde (Sigma-Aldrich) in PBS for 1 day, and decalcified in 10% ethylenediaminetetraacetic acid for 1 week. The paraffin-embedded specimens were sliced into 4 μm sections, mounted on silane-coated slides, stained with Haematoxylin and Eosin (HE), and observed under a light microscope (Leica Microsystems, Bannockburn, IL). The Rosenthal's canal was divided into three regions: apical, middle and basal and the three regions were used for evaluation of cochlear histology. We used five mice per group for histopathological assessment. In each mouse, we evaluated every third modiolar section obtained from one unilateral cochlea for a total of ten sections. Tissues from the same animals were used for neuron counting and hair cell counting.

Neuron Counting

Spiral ganglion neurons were counted in the apical, middle, and basal regions of the cochlear sections using a 20X objective as previously described (Someya et al., 2009). The corresponding area of Rosenthal's canal was measured on digital photomicrographs of each canal profile. The perimeter of the canal was traced with a cursor using ImageJ software (Rasband, W.S., ImageJ, U.S. National Institutes of Health, Bethesda, Maryland, USA, <http://rsb.info.nih.gov/ij/>, 1997–2007). The computer then calculated the area within the outline. The numbers of neurons were determined as the number of neurons per mm². Ten sections of the unilateral apical, middle, and basal turns were evaluated in one cochlea per mouse.

Hair Cell Counting

OH cells and IH cells were counted in the apical, middle, and basal regions of the cochlear sections using a 40X objective as previously described (Someya et al., 2009). Hair cells were identified by the presence of a nucleus. The OH cell survival % was calculated as the number of intact OH cells present out of the three OH cells which should be observed in each turn of one cochlea in tissue sections of mice with normal hearing. The IH cell survival % was calculated as the number of intact IH cells present out of the one IH cell which should be observed in each turn of one cochlea in tissue sections of mice with normal hearing. Ten sections of the unilateral apical, middle, and basal turns were evaluated in one cochlea per mouse.

Isolation of Mitochondria

Mice at 5 months of age were sacrificed by cervical dislocation and inner ear (cochlea vestibular), neocortex, and liver were quickly removed and placed in ice-cold Tris buffer (10 mM Tris, 1 mM EDTA, 1 μ g/ml aprotinin, 1 μ g/ml leupeptin, 1 μ g/ml phenylmethanesulfonyl fluoride, pH 7.4). Tissues were homogenized in ice-cold hypotonic Tris buffer (320 mM sucrose, 10 mM Tris, 1 mM EDTA, 1 μ g/ml aprotinin, 1 μ g/ml leupeptin, 1 μ g/ml phenylmethanesulfonyl fluoride, PH 7.4) on ice using a tissue grinder. The homogenate was centrifuged at 600 \times g for 5 min at 4°C. The supernatant was then centrifuged at 12,000 \times g for 10 min at 4°C and the supernatant was discarded. The pellet was resuspended in 1 ml of the Tris buffer and centrifuged 12,000 \times g for 10 min at 4°C, and the supernatant was discarded. For mitochondrial lysate preparation, the pellet was resuspended in 400 μ l of 1% NP40 buffer (1% NP40, 250 mM NaCl, 50 mM Tris, 1 mM EDTA, 1 μ g/ml aprotinin, 1 μ g/ml leupeptin, 1 μ g/ml phenylmethanesulfonyl fluoride, pH 7.4), incubated for 30 min at 4°C, and centrifuged at 12,000 \times g for 10 min at 4°C. The supernatant was used as mitochondrial lysate for the Idh2 and NADPH assay. The protein contents of the mitochondria lysates were determined by the Bradford method using the Bio-Rad Protein assay, according to the manufacturer's instructions (Bio-Rad, Hercules, CA).

Measurement of NADPH

NADPH levels were determined by the method of Zerez et al. (Zerez et al., 1987). Briefly, 200 μ l of the mitochondrial lysate was mixed with 180 μ l of a nicotinamide solution (10 mM nicotinamide, 20 mM NaHCO₃, 100 mM Na₂CO₃) and freeze-thawed three times to extract NADP⁺ and NADPH. To destroy NADP⁺ in the sample, 90 μ l of the lysate was incubated in a heating block for 30 min at 60°C. Twenty five microliters of each unheated and heated sample was mixed with 225 μ l of a reaction mixture (100 mM Tris, 5 mM EDTA, 0.5 μ M thiazolyl blue tetrazolium bromide, 2 μ M phenazine ethosulfate, 1.3 units glucose-6-phosphate dehydrogenase, pH 8.0) and incubated in a water bath for 5 min at 37°C. The reaction mixture was then transferred to each well of a 96-well plate and 1 μ l of 1 mM glucose-6-phosphate was added in each well to start the reaction. The absorbance was read at 570 nm every 10 s for 3 min in a microplate reader (Bio-Rad, Hercules, CA). All samples were run in duplicate. The reaction rates were calculated and NADPH levels were determined as the ratio of NADPH (heated sample) to the total of NADP⁺ and NADPH (unheated sample).

Coimmunoprecipitated Assay

IDH2 and Sirt3 were cotransfected into HEK293 cells and cell lysates were immunoprecipitated with IgG antibody or FLAG beads overnight at 4°C, then boiled with SDS loading buffer and subjected to Western blotting. IDH2-FLAG, Sirt3-HA, Sirt3-FLAG, IDH2-MYC were detected as indicated.

Generation of Stably Transfected Cell Pools

The EcoRI-Sall fragment containing the IDH2-Flag cDNA was subcloned from plasmid pCDNA 3.1-IDH2-Flag into the EcoRI-Sall site of pBabe-puro (Lei, et al., 2008). HEK293 cells were initially cultured in DMEM supplemented with 10% FBS prior to their use in establishing stable transfections. To establish stable IDH2-expressing cells, pBabe-IDH2-FLAG retroviruses were generated and used to infect HEK293 cells. Stable pools were selected with puromycin (1.5 μ g/ml) for 5 days. To establish stable Sirt3-expressing cells, HEK293 cells were transfected with pCDNA3-Sirt3-FLAG. A vector control cell line was established by the same method using pCDNA3. Simultaneous expression of Sirt3 and IDH2 was achieved by transfection of pCDNA3-Sirt3 into stable expressed IDH2 HEK293 cells. After transfection, cells were selected in the medium containing G418 (1.5 mg/ml) for 10 days. The antibiotic-resistant clones were selected, expanded, and further cultured in medium supplemented with adequate amounts of antibiotics. Cell lysate were used to measure the NADPH concentrations.

Cytotoxicity Assay

The four stable cell pools (vector, Sirt3, Idh2 and Sirt3-Idh2 lines) were first grown on a 96 well plate at a density of 1 \times 10⁴ cells/well, overnight before oxidant treatment and subsequent assessment of cell viability, using 3-(4,5-dimethylthiazol-2-yl)-2,5-diphenyltetrazolium bromide (MTT) assay (Di Matteo et al., 1997). After overnight culture, 25 μ M menadione or 1mM hydrogen peroxide were applied to the cells in serum free DMEM, and cells were incubated for additional 48 hr at 37°C. After 48 hr of oxidant treatment, culture media were aspirated under vacuum, before 200 μ l of MTT (1 mg/ml) was added and further incubated for 4 hr at 37°C. The MTT solution was discarded by aspirating, and then the resulting formazan product converted by the viable cells was dissolved in 150 μ l dimethylsulfoxide. The absorbance was read in an ELISA plate reader at 595 nm. Cell viability is expressed as a percentage of the absorbance measured in the untreated control cells.

SUPPLEMENTAL REFERENCES

Di Matteo, M.A., Loweth, A.C., Thomas, S., Mabley, J.G., Morgan, N.G., Thorpe, J.R., and Green, I.C. (1997). Superoxide, nitric oxide, peroxynitrite and cytokine combinations all cause functional impairment and morphological changes in rat islets of Langerhans and insulin secreting cell lines, but dictate cell death by different mechanisms. *Apoptosis* 2, 164–177.

Lei, Q.Y., Zhang, H., Zhao, B., Zha, Z.Y., Bai, F., Pei, X.H., Zhao, S., Xiong, Y., and Guan, K.L. (2008). TAZ promotes cell proliferation and epithelial-mesenchymal transition and is inhibited by the hippo pathway. *Mol. Cell. Biol.* 28, 2426–2436.

Someya, S., Xu, J., Kondo, K., Ding, D., Salvi, R.J., Yamasoba, T., Rabinovitch, P.S., Weindruch, R., Leeuwenburgh, C., Tanokura, M., and Prolla, T.A. (2009). Age-related hearing loss in C57BL/6J mice is mediated by Bak-dependent mitochondrial apoptosis. *Proc. Natl. Acad. Sci. USA* 106, 19432–19437.

Zerez, C.R., Lee, S.J., and Tanaka, K.R. (1987). Spectrophotometric determination of oxidized and reduced pyridine nucleotides in erythrocytes using a single extraction procedure. *Anal. Biochem.* 164, 367–373.

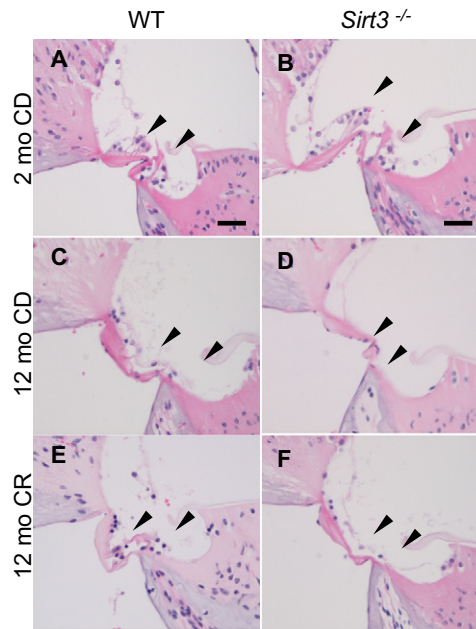


Figure S1. Histopathology, Related to Figure 1

(A–F) Basal cochlear regions from control diet WT and *Sirt3*^{-/-} mice at 2 months of age (A and B) and 12 months of age (C and D), calorie-restricted WT, and *Sirt3*^{-/-} mice at 12 months of age (E and F) (n = 5). Arrows indicate hair cell regions. Scale bar = 20 μ m. CD = control diet, CR = calorie restricted diet.

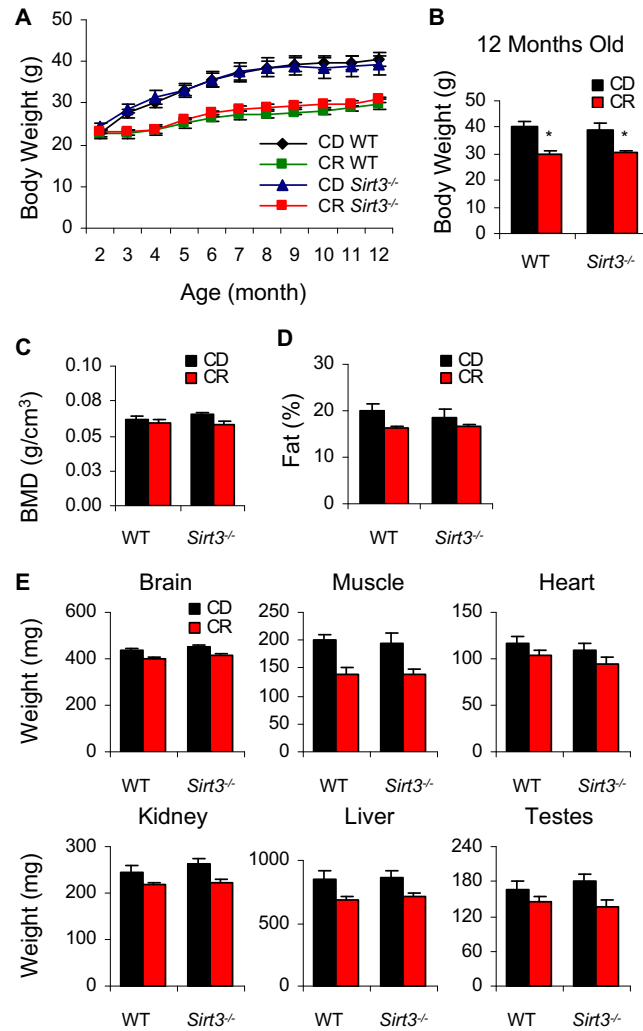


Figure S2. Body Weight, BMD, Total Body Fat Percentage, and Tissue Weight, Related to Figure 1

(A and B) Body weight was measured from control diet and calorie restricted WT and *Sirt3*^{-/-} mice every month from 2 month of age until 12 month of age (A) and at 12 month of age (B) (n = 10–12).

(C and D) Bone mineral density (BMD) (C) and total body fat percentage (D) were calculated from control diet and calorie restricted WT and *Sirt3*^{-/-} mice at 5 month of age (n = 5).

(E) Tissue weight was measured from control diet and calorie restricted WT and *Sirt3*^{-/-} mice at 5 month of age (n = 10–12). *Significantly different from control diet mice (p < 0.05).

Data are means ± SEM.

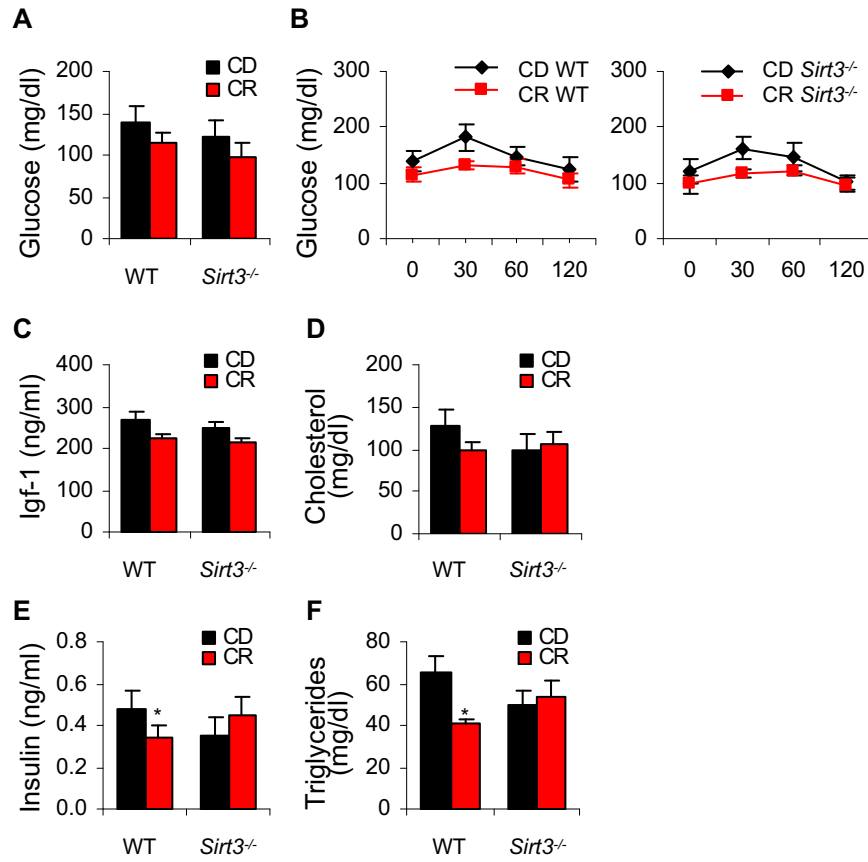


Figure S3. Serum Glucose Levels, Glucose Tolerance, Serum Insulin, Triglycerides, Igh-1, and Cholesterol Levels, Related to Figure 1

(A) Serum glucose levels of control diet and calorie-restricted WT and *Sirt3*^{-/-} mice at 5 month of age (n = 5–7).

(B) Serum glucose levels were measured in control diet and calorie restricted WT and *Sirt3*^{-/-} mice at 5 month of age at 0, 30, 60, and 120 min after glucose injection (n = 5–7).

(C–F) The contents of serum insulin (C), triglycerides (D), Igf-1 (E), and cholesterol (F) were measured from control diet and calorie-restricted WT and *Sirt3*^{-/-} mice at 5 month of age (n = 7–11).

Data are means ± SEM.

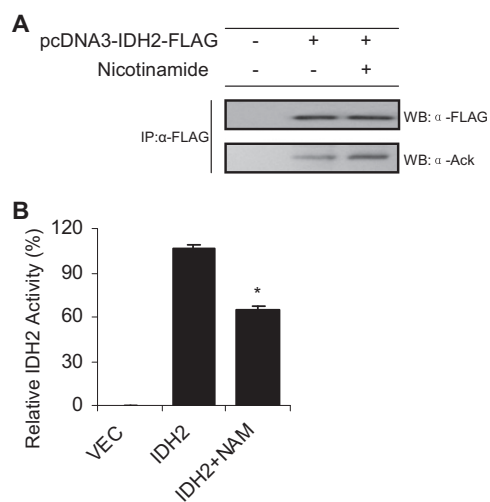


Figure S4. Nicotinamide Increases IDH2 Acetylation Levels and Decreases Its Activity, Related to Figure 5

(A and B) IDH2 was overexpressed in HEK293 cells following 5 mM nicotinamide treatment for 16 hr. Cell lysates were immunoprecipitated with anti-FLAG beads at 4°C overnight followed by western blotting with anti-FLAG antibody or anti-acetyl-lysine antibody (A). (B) Quantification of IDH2 activities from A (n = 3). NAM = nicotinamide. Data are means \pm SEM.